Colloid Polym Sci (2003) 282: 170–176
DOI 10.1007/s00396-003-0929-7

ORIGINAL CONTRIBUTION

Graciela Alimenti
Paula Messina
Marcela A. Morini
Pablo C. Schulz

Evaporation studies on sodium dehydrocholate aqueous solutions

Received: 10 March 2003
Accepted: 16 April 2003

G. Alimenti · P. Messina · M.A. Morini
P.C. Schulz (✉)
Departamento de Química e Ingeniería
Química, Universidad Nacional del Sur,
8000 Bahía Blanca, Argentina
E-mail: pschulz@criba.edu.ar
Fax: +54-291-4551447

Abstract The evaporation through the air/solution interface of sodium dehydrocholate (NaDHC) aqueous solutions was studied by surface tension and microbalance measurements. The evaporation rate was related to the aggregation processes in the bulk, but not with the adsorption monolayer compactness. Except for very dilute solutions the air/solution interface was saturated by NaDHC molecules, giving rise to a strongly nonideal monolayer. At very low concentration, the adsorbed monolayer behaved as an ideal two-dimensional gas. The results were in agreement with previous research results.

Keywords Sodium dehydrocholate
Evaporation · Air/water interface
Adsorption

Introduction

Bile salts are natural surfactants mainly stored in the gall bladder. Their function is essentially the emulsification and transport of food fats and lipids. The physicochemical properties of bile salts are of interest because of their very important role in the metabolic process of absorption at intestinal level. The solution behaviour of bile salts is considerably different from that of ordinary surfactants having a long alkyl chain and a hydrophilic head group [1, 2, 3].

Bile salts are different to common surfactants, which in general have their polar headgroup attached to a flexible hydrocarbon chain. Bile salts have a rigid steroid backbone, having up to three hydroxyl groups and a branched linear chain ended by a carboxylate group, which may or may not be conjugated with glycine or taurine. This difference in structure generates atypical aggregation behaviour.

From the point of view of surfactant physical chemistry, bile salts are far from being as studied as the more traditional structured surfactants. For the same bile salt there is a large dispersion of data leading to contradictory conclusions.

Some authors found that most of the physicochemical properties of aqueous bile salts undergo important changes at several concentrations. These changes have been interpreted as arising from a stepwise aggregation process. As an example, at least three aggregation steps were reported in sodium cholate aqueous solutions [4, 5].

Evaporation is an active research field. It has been investigated in pure liquids [6], microemulsions [7, 8], and through insoluble surfactant monolayers [9, 10, 11, 12]. Recently, computer simulations were performed [13, 14, 15, 16, 17, 18]. The evaporation through soluble surfactant monolayers was also studied [19, 20, 21]. In these studies, it was found that the evaporation rate through soluble surfactant monolayers only depended on bulk water activity. No dependence on the state of the adsorbed layer was found.

In preceding works we studied the aggregation of sodium dehydrocholate (NaDHC) by a battery of methods [22, 23, 24, 25]. In this work we studied the effect of the NaDHC aggregation in water on the solution evaporation. NaDHC is a scarcely studied surfactant derived from bile salt, which adds interest to this work. As far as we know, this is the first study of steroid surfactants of this kind. The information derived from these measurements may be useful to complete the knowledge of the complex aggregation behaviour of bile salts and related compounds.

Experimental

Dehydrocholic acid (HDHC) was from Dr. Theodor Schuchardt (Munich) and was of analytical grade. A concentrated NaDHC aqueous solution was prepared by weighing a quantity of HDHC and by dissolution in an appropriate amount of concentrated NaOH solution. Then the solution was diluted to obtain the desired concentrations. Only double-distilled water was used.

Surface tension was measured with a ring tensiometer (Krüss) at 25 °C. The evaporation rate was measured using a Cahn-1000 electrobalance with continuous recording. The data were recorded at 20 cm h^{-1} and 1 mg full scale. Each experiment was run twice. Measurements were made at 18 and 28 °C and at atmospheric external pressure.

Theory

Surface tension measurements together with ion-selective electrode measurements enable the determination of the area occupied by one molecule of surfactant at the air/water interface. The area per molecule of pure surfactant, a_S, may be computed from the surface tension plot of NaDHC solutions, using the Gibbs equation [26]:

$$\Gamma_S = -\frac{1}{RT} - \frac{\partial\sigma}{\partial \ln\, a_{\text{salt}}}, \tag{1}$$

where $a_{\text{salt}} = a_- a_+$ is the activity of the absorbable salt, a_- and a_+ being the activities of free surfactant anion and counterion, respectively, determined by using the appropriate ion-selective electrodes. Only the free (non-micellised) Na^+ and DHC^- ions may adsorb at the air/solution interface. Micelles are not surface-active [27] and are excluded from the interface region [28]. These data were obtained from the literature [23]. The relationship $a_S = (\Gamma_S N_A)^{-1}$ gives the area per adsorbed surfactant molecule.

The loss of weight (in kilograms per square meter per second) gives curves following parabolic equations with time having the general form [8]

$$v = v_0 - Kt^{1/2}, \tag{2}$$

where v and v_0 are the rate of evaporation at time t and the initial evaporation rate, measured in loss of mass per area unit and per second. The values of v_0 and K are found by the least-squares linear regression method.

The only hindrance for the initial rate of evaporation, v_0, is the reluctance of the molecules of the evaporating substance (water) to leave the surface in the initial state of equilibrium, which is related to the evaporation enthalpy [8]. The K coefficient is related to the rate of diffusion of molecules with sufficient energy to evaporate, from the bulk to the surface, where the initial evaporation created a deficit of energetic molecules.

The activation energy of v_0 and K may be computed from the slope of the Arrhenius relation:

$$\ln(v_0 \text{ or K}) = -\frac{E_a}{RT} + \text{constant}. \tag{3}$$

McCoy [12], using the mass-transfer model of Nguyen et al. [29], found the following relation for the evaporation through the air/water interface:

$$Q_w = 2(D_s t/\pi)^{1/2}(p^*/RT - c_i), \tag{4}$$

where Q_w is in moles per metre squared per second, D_s is the water diffusivity in air (3×10^{-5} m^2 s^{-1}) [12], p^* is the vapor pressure of water at the temperature of the experiment, and c_i is the initial concentration of water in the gaseous phase.

By comparison of Eqs. (2) and (4) it may be seen that

$$K\left(\text{kg m}^{-2}\ \text{s}^{-3/2}\right) = 2M_w(D_s/\pi)^{1/2}(p^*/RT - c_i), \tag{5}$$

where M_w is the molar mass of water. The value of c_i depends on the experimental conditions, and it may be determined by measurements on pure water.

Results

A series of evaporation measurements at 18 °C is shown in Fig. 1. The results of surface tension measurements are shown in Fig. 2.

Discussion

NaDHC aggregates by a stepwise mechanism [22]. Below $c_1 = (10.1 \pm 4.5)\text{x}10^{-4}$ mol dm^{-3} there is a molecular solution with some strongly insoluble HDHC produced by hydrolysis. Between c_1 and $c_2 = (2.0 \pm 2.2)\text{x}10^{-3}$ mol dm^{-3}, an acid-soap-like complex (NaDHC.HDHC) appears and the amount and the aggregate's size increase with concentration above c_2. At $c_3 = (2.28 \pm 0.55)\text{x}10^{-2}$ mol dm^{-3} true micelles form. These micelles increase in size with concentration and change their shape at $c_4 = 8\text{x}10^{-2}$ mol dm^{-3}, giving nonsymmetrical micelles.

By using the activities of free ions from the literature [23], the relationship between the surface tension, σ, and the Naperian logarithm of the activity of free salt ($a_- a_+$) was drawn (Fig. 3). From this graph, the area per surfactant molecule adsorbed at the air/water interface was determined and is represented in Fig. 4.

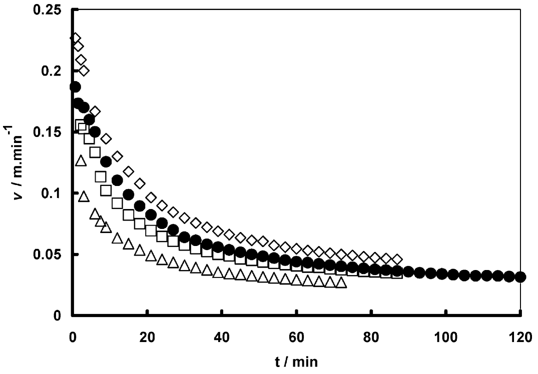

Fig. 1 Evaporation rate at 18 °C of pure water (*diamonds*), 0.04 mol dm^{-3} sodium dehydrocholate (*NaDHC*) (*squares*), 0.06 mol dm^{-3} NaDHC (*circles*) and 0.1 mol dm^{-3} NaDHC (*triangles*)

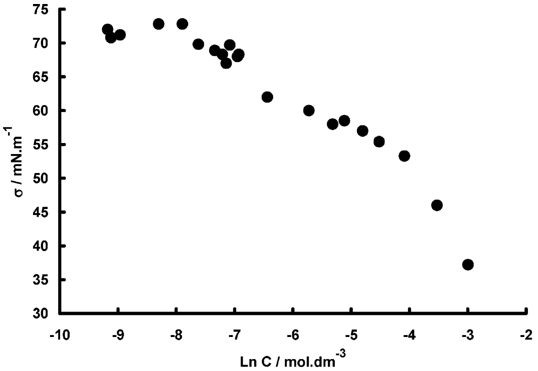

Fig. 2 Surface tension of aqueous NaDHC solutions as a function of the natural logarithm of the total concentration at 25 °C

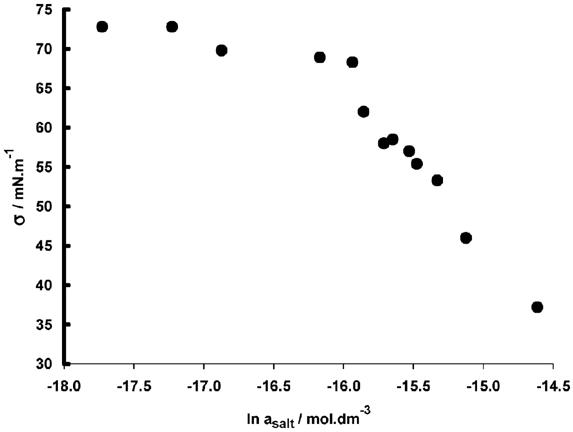

Fig. 3 Surface tension of aqueous NaDHC solutions versus the natural logarithm of the activity of free (nonaggregated) surface-active salt at 25 °C

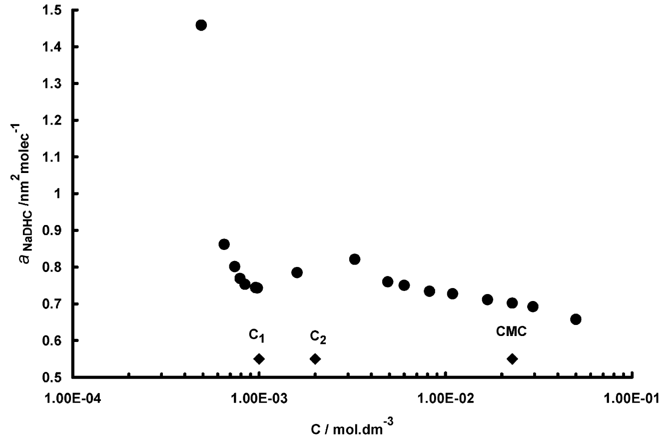

Fig. 4 The area per adsorbed molecule at the air/solution interface, as a function of the NaDHC total concentration at 25 °C. The different aggregation concentrations are represented by *diamonds*

From the literature, the area per NaDHC molecule adsorbed at the critical micelle concentration (cmc) was $a_{\mathrm{NaDHC}} = 0.702$ nm^2 [24]. On the basis of the structure of the DHC$^-$ ion, which may be roughly considered as a rectangular plate of 0.571-nm width and 1.286-nm length [30], the computed value of a_{NaDHC} was 0.735 nm^2. Therefore, the experimental value may be explained by the accommodation of the molecule with its plane lying parallel to the water surface. This situation allows the three carbonyl groups in the hydrocarbon backbone to form hydrogen bonds with water [24]. Some literature values of the limiting area at collapse pressure for bile salt monolayers are 1.08 nm^2 (cholic acid), 0.80 nm^2 (chenodeoxycholic acid) and 0.73 nm^2 (ursodeoxycholic acid) [31]. The similarity of the preceding areas with that of NaDHC suggested that the monolayer adsorbed at the air/water interface at the cmc was very compact. Other bile salts show less compact monolayers at the cmc with an area per molecule of 1.48 nm^2 (sodium cholate) and 2.23 nm^2 (sodium deoxycholate) [32].

It may be seen in Fig. 4 that on increasing the NaDHC concentration the solution surface is saturated with surfactant molecules at the concentration c_1 at which the acid-soap-like complex begins to form [22]. The increase in the a_{NaDHC} value between c_1 and 0.00326 mol dm^{-3} may be due to an energetic advantage of the acid-soap-like complex compared with the adsorbed state. Above this concentration, there is a slow increase in the adsorption, leading back to the saturation of the surface.

The product πa_{NaDHC} versus π is shown in Fig. 5, $\pi = \sigma_0 - \sigma$ being the surface pressure. This figure is the two-dimensional analogue to the *pv* versus *v* graph for three-dimensional fluids. The ideal value for a two-dimensional gas is $kT = 4$ mN nm^2 m^{-1} at 25 °C. It may be seen that the adsorbed monolayer behaved as an ideal two-dimensional gas at concentrations below c_1. Above this concentration, the adsorbed monolayer was strongly nonideal, showing a strong resistance to the reduction in a_{NaDHC}, especially slightly above c_2.

These results suggest that once the surface of the solution is covered by the NaDHC molecular plane lying parallel to the water surface, with their carbonyl groups in contact with water, it is very difficult to produce a further reduction of a_{NaDHC}. The origin of this resistance may be that a subsequent reduction in the area per adsorbed molecule may only be obtained by accommodation of the molecular plane perpendicular to the solution surface, and this position removes the contact among carbonyl groups and water. This "dehydration" of the carbonyl groups may require an excessive amount of energy.

The relation between the initial evaporation rate, v_0, and the total concentration of NaDHC at 18 and 28 °C is given in Fig. 6. Both curves are almost parallel. The only hindrance for v_0 is the reluctance of the molecules of the evaporating substance (water) to leave the surface in the initial state of equilibrium, which is related to the evaporation enthalpy [8]. In turn, this thermodynamic property is related to the activity of water and, thus, to the concentration of particles in solution. There is a decrease in the initial evaporation rate between c_2 and the cmc, which indicates an increase in the concentration of particles in solution; however, this decrease is slower than that below c_1. (The values for pure water were 1.09 and 1.21 mg cm^{-2} s^{-1} at 18 and 28 °C, respectively.) This is a consequence of the formation of the acid-soap-like complex:

$$\mathrm{Na^+ + 2DHC^- + H_2O \leftrightarrow HNaDHC_2 + OH^-}$$

The number of particles in solution is smaller than the number of ions added to the solution. At the cmc there is an increase in v_0 because the formation of micelles produces an additional reduction in the number of independent particles in solution, but a subsequent increase in the total concentration produces an increase in the micelle concentration, and thus a reduction in v_0.

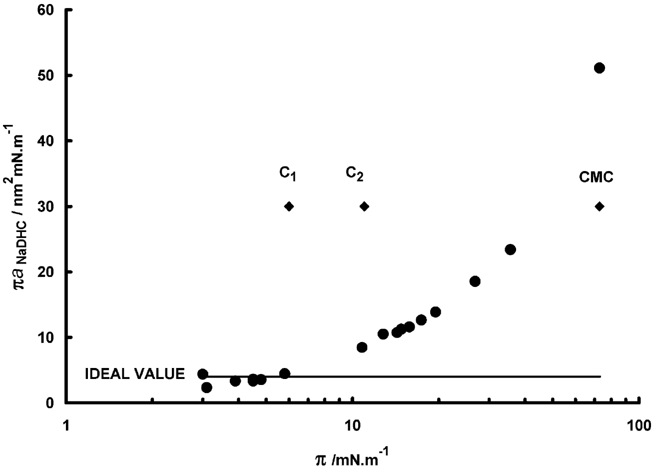

Fig. 5 The area per adsorbed molecule–surface pressure product versus the surface pressure for aqueous NaDHC solutions at 25 °C. The different aggregation concentrations are represented by *diamonds*

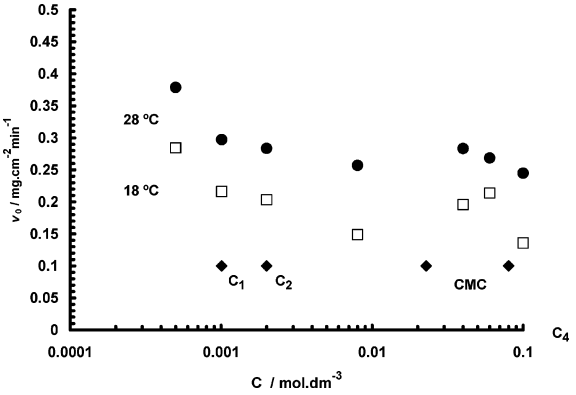

Fig. 6 The initial rate of evaporation of aqueous NaDHC solutions at 18 °C (*squares*) and 28 °C (*circles*).The different aggregation concentrations are represented by *diamonds*

The dependence of the activation energy of v_0 computed with Eq. (3) is shown in Fig. 7. $E_{a(v0)}$ of all solutions is higher than the value for water (7.59 kJ mol^{-1}). There is a minimum in the range c_1–c_2, followed by an increase when acid-soap-like aggregates formed, and a reduction when micelles appeared. There is an increase above c_4.

The dependence of K on the total concentration at 18 and 28 °C is shown in Fig. 8. The values for pure water were K=0.267 and 0.295 mg cm^2 s$^{-3/2}$at 18 and 28 °C, respectively. Above c_2 both curves are almost coincident, showing a decrease until the cmc is reached. Then, there is an increase in K, followed by a decrease above c_4. An increase in the concentration of the particles in solution must produce a hindrance in the diffusivity of water molecules from the bulk to the surface, and this situation is reflected in the variation of $K(c)$. The explanation is the same as in the dependence of v_0 on c. The difference between the two curves below c_2 may be due to the increase in hydrolysis of NaDHC at the higher temperature, producing insoluble HDHC that may interfere less with the diffusion of water. When an acid-soap-like complex is formed at c_2, both curves become almost the same.

The activation energy for K is shown as a function of c in Fig. 9. The $E_{a(K)}$ value is higher than that of pure water (7.27 kJ mol^{-1}) at low total concentration, but only when acid-soap-like aggregates formed at c_2, $E_{a(K)}$ became smaller than the pure water value, and only increases above c_4. Anisometric micelles formed at this concentration.

At very low concentrations NaDHC behaves as a water-structure breaker [22]; thus, the reduction in the

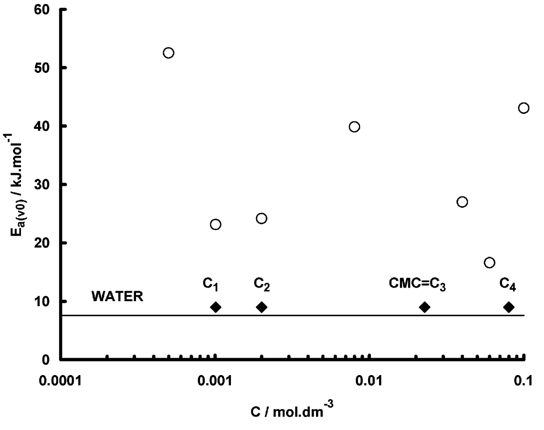

Fig. 7 The activation energy of the initial rate of evaporation of aqueous NaDHC solutions. The *horizontal line* indicates the pure water value, and the different aggregation concentrations are represented by *diamonds*

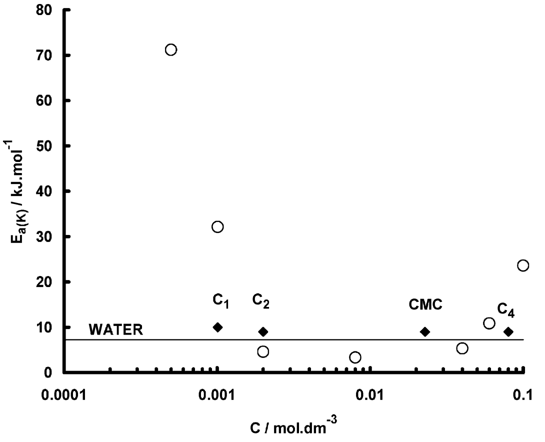

Fig. 9 The activation energy of K (Eq. 2) of aqueous NaDHC solutions. The *horizontal line* indicates the pure water value, and the different aggregation concentrations are represented by *diamonds*

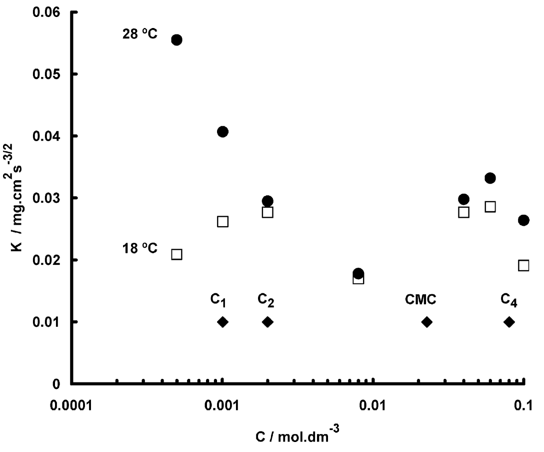

Fig. 8 The value of K (Eq. 2) of aqueous NaDHC solutions at 18 °C (*squares*) and 28 °C (*circles*). The different aggregation concentrations are represented by *diamonds*

$E_{a(K)}$ value may be explained on the basis of the theory developed by Némethy and Scheraga for hydrophobic hydration [33, 34, 35, 36, 37]. The structure of the hydrocarbon hydration cages is affected by the solubilised hydrocarbon size and shape, and some hydrocarbons which may not enter the hydrophobic hydration cages act as structure breakers [38, 39, 40, 42]. In addition, the hydration of charged polar groups, that of the uncharged polar groups and the hydrophobic hydration are mutually incompatible. Which of them will predominate depends on the solute molecule's structure: the size and shape of the hydrocarbon backbone, and the kind and localisation of the hydrophilic groups. The large size and the stiffness of the steroid backbone and the presence of the polar groups (three carbonyl and one carboxyl) in different parts of the molecule, hindered the formation of a structured water cage surrounding the surfactant molecule and favoured the destruction of the "icebergs". This increased the number of "free" (less hydrogen-bonded) water molecules that need less energy to diffuse to the surface than those in pure water, in spite of the structure-making effect of Na^+ and OH^- ions. At very low concentration, the structure-making effect of the small ions may be predominant, and at c_4, the large micelles may eliminate enough DHC^- ions from water contact to make the effect of the structure-making ions predominant again.

The dependence of the $(p_0^*-p^*)/p_0^*$ ratio at 18 and 28 °C is depicted in Fig. 10, p_0^* being the vapour pressure of pure water. The vapour pressure at 18 °C decreased up to c_2, and then there was a slight increase and then a decrease between the cmc and c_4. The decrease is caused by a rise in the number of particles in solution with the total concentration, but at c_2 a large proportion of the added particles form aggregates. Thus, the number of effective particles affecting the colligative properties of water was much smaller than the nominal one, and p^* increased. Since micelles are ionised but the acid-soap-like complex is not, and at the cmc the number of particles must increase and p^* decrease. The behaviour at 28 °C above c_2 was the same; however, there was a difference below this concentration, because there was an increase in p^* with concentration. This may reflect the formation of the acid-soap-like complex at a lower concentration when the temperature was increased.

A comparison of the evaporation, the vapour pressure and the adsorption results shows that the degree of coverage of the solution surface by surfactant molecules did not affect the evaporation or the vapour pressure. As was stated for more conventional soluble surfactant solutions [19, 20, 21], the state of the surface

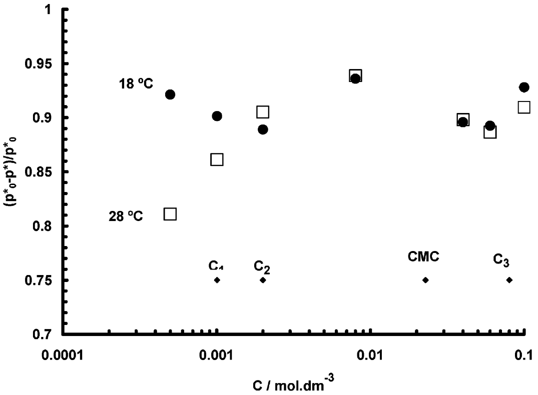

Fig. 10 The relative decrease in vapour pressure versus the total concentration of aqueous NaDHC solutions. The different aggregation concentrations are represented by *diamonds*

monolayer did not affect these properties, in spite of the very different structure of this interface. The saturated monolayer of NaDHC is permeable enough to water molecules to avoid the evaporation hindrance observed when insoluble monolayers are spread on water. Evaporation and vapour pressure changes were affected only by the transformations occurring in the bulk solution.

Conclusions

1. NaDHC molecules, giving rise to a strongly nonideal monolayer once the acid-soap-like complex has formed, rapidly saturate the air/solution interface. Below this concentration, the surface is not saturated and behaves as an ideal two-dimensional gas.
2. The evaporation rate of NaDHC solutions is not affected by the degree of coverage of the surface.
3. The changes in the initial rate of evaporation and the diffusivity of water from the bulk to the solution surface are related to the changes in surfactant aggregation.
4. The activation energy of the initial evaporation rate in solutions is higher than that of pure water, and follows the changes in the activity of water, which in turn is related to the changes in surfactant aggregation. The activation energy of water diffusivity from the bulk to the solution surface in some solutions is lower than that of pure water, reflecting the structure-breaking nature of NaDHC.

Acknowledgements P.M. has a fellowship of the Consejo Nacional de Investigaciones Científicas y Técnicas de la República Argentina. This work was supported by a grant of the Universidad Nacional del Sur.

References

1. Krathovil JP (1984) Hepatology 4:855
2. Attwood D, Florence AT (1983) Surfactant systems, their chemistry, pharmacy and biology. Chapman & Hall, New York p 185
3. Lichtenberg D, Robson RJ, Dennis EA (1983) Biochim Biophys Acta 737:285
4. Fontell K (1971) Kolloid Z Z Polym 244:246
5. Fontell K (1971) Kolloid Z Z Polym 246:710
6. Yen SM, Ytrehus T (1981) Chem Eng Commun 10:357
7. Friberg SE, Yu B, Lin JW-P, Barni E, Young T (1993) Colloid Polym Sci 271:152
8. Schulz PC, Gschaider de Ferreira ME, Sierra GL (1995) Colloid Polym Sci 273:439
9. Blank M, Mussellwhite PR (1968) J Colloid Interface Sci 27:188
10. Deryaguin V, Bakanov SP, Kurgin IS (1960) Discuss Faraday Soc 30:96
11. Deryaguin V, Bakanov SP, Kurgin IS (1961) Colloid J USSR 23:222
12. McCoy BJ (1988) AIChE J 28(5):844
13. Yasuoka K, Matsumoto M, Kataoka Y (1994) J Chem Phys 101(9):1
14. Matsumoto M, Yasuoka K, Kataoka Y (1993) Thermal Sci Eng 2:64
15. Matsumoto M, Yasuoka K, Kataoka Y (1994) J Chem Phys 101(9):9
16. Matsumoto M, Kataoka Y (1992) Phys Rev Lett 69:3782
17. Matsumoto M, Kataoka Y (1994) Mol Simul 12:211
18. Yasuoka K, Matsumoto M, Kataoka Y (1994) Bull Chem Soc Japan 67:859
19. Schulz PC, Morini MA, Gschaider de Ferreira ME (1998) Colloid Polym Sci 276:92
20. Schulz PC, Minardi RM, Gschaider de Ferreira ME, Vuano B (1998) Colloid Polym Sci 276:52
21. Lickenheimer K, Zembala M (1997) J. Colloid Interface Sci 188:363
22. Messina P, Morini MA, Schulz PC, Ferrat G (2002) Colloid Polym Sci 280:328
23. Schulz PC, Messina P, Morini MA, Vuano B (2002) Colloid Polym Sci 280:1104
24. Messina P, Morini MA, Schulz PC (2003) Colloid Polym Sci DOI 10.1007/s00396-002-0853-2
25. Messina P, Morini MA, Schulz PC (submitted)
26. Schulz PC, Morini MA, Gschaider de Ferreira ME (1998) J Colloid Polym Sci 276:232
27. Shaw JD (1970) Introducción a la química de superficies y coloides. Alhambra, Madrid
28. Lu JR, Simister EA, Thomas RK, Penfold J (1993) J Phys Chem 97:13907
29. Nguyen L, Carbonell RG, McCoy BJ (1979) AIChE J 25:1015
30. Sugihara G, Tanaka M (1978) Hyomen 16:537

31. Miyoshi H, Nagadome S, Sugihara G. Kagimoto H, Ikawa Y, Igimi H, Shibata O (1992) J Colloid Interface Sci 194:216
32. Roy BK, Moulik SP (1996) J Surf Sci Technol 12:86
33. Némethy G, Scheraga HA (1962) J Chem Phys 36:3382
34. Némethy G, Scheraga HA (1962) J Chem Phys 36:3401
35. Klotz IM (1960) In: Protein structure and function. Brookhaven symposium in biology 13:25
36. Klotz IM (1958) Science 128:815
37. Kauzmann W (1959) Adv Protein Chem 14:1
38. Bernal ID, Fowler RH (1963) J Chem Phys 39:2035
39. Frank HS, Evans MW (1945) J Chem Phys 13:507
40. Claussen WF, Polglash MF (1952) J Am Chem Soc 74:4817
41. Glew DN, Moelwyn EA (1953) Discuss Faraday Soc 15:150
42. Glew DN (1962) J Phys Chem 66:605